DOI: 10.1021/ic100975x

Inorganic Chemistry
Article

$Yb_3AuGe_2In_3$: An Ordered Variant of the YbAuIn Structure Exhibiting Mixed-Valent Yb Behavior

Maria Chondroudi,[†,§] Sebastian C. Peter,[⊥] Christos D. Malliakas,[⊥] Mali Balasubramanian,[‡] Qing'An Li,[†] and Mercouri G. Kanatzidis*[,†,⊥]

[†]*Materials Science Division, and* [‡]*Advanced Photon Source, Argonne National Laboratory, Argonne, Illinois 60439, United States,* [§]*Department of Chemistry, Michigan State University, East Lansing, Michigan 48824, United States, and* [⊥]*Department of Chemistry, Northwestern University, Evanston, Illinois 60208-3113, United States*

Received May 16, 2010

$Yb_3AuGe_2In_3$ was obtained as large single crystals in high yield from reactions run in liquid indium. Single crystal X-ray diffraction data show that $Yb_3AuGe_2In_3$ is an ordered variant of YbAuIn with lattice constants, $a = b = 7.3153(8)$ Å and $c = 4.4210(5)$ Å, and space group $P\bar{6}2m$. The parent compound YbAuIn was also studied for comparison. YbAuIn crystallizes in the ZrNiAl structure type, hexagonal, $P\bar{6}2m$ space group with lattice parameters $a = b = 7.7127(11)$ Å and $c = 4.0294(8)$ Å. In $Yb_3AuGe_2In_3$, Ge substitutes for one of the two Au positions in the ternary compound $Yb_3Au_3In_3$. The structure can be described as alternating $[Ge_2In_3]$ and $[Yb_3Au]$ slabs that stack along the *c*-axis. The magnetic susceptibility data follow a modified Curie−Weiss law. The effective magnetic moment μ_{eff} of 0.52 μ_B/Yb atom was deduced from the Curie constant and Curie−Weiss constant of $\theta_p = -1.5$ K indicating antiferromagnetic interactions in $Yb_3AuGe_2In_3$. X-ray absorption near edge spectroscopy (XANES) measurements indicate intermediate valency for Yb in both compounds. The metallic nature of both compounds was confirmed by the resistivity measurements. Specific heat data for $Yb_3AuGe_2In_3$ and YbAuIn give an electronic γ term of 31 and 84 mJ/mol·K^2, respectively, suggesting that the ternary analog is a "light" heavy fermion compound.

1. Introduction

Intermetallic compounds of the ternary systems RE/T/In (T = Cu, Ag, Au) include numerous new phases that exhibit rich structural variety[1,2] and interesting physical properties.[3] Some examples are CeAuIn,[4−8] the families of REAuIn (RE = Eu, Gd−Ho, Yb),[4,7,9−13] and $REAu_2In$.[11,14−18] In the $REAu_2In$ family, the members formed by light RE (La−Sm) elements undergo a structural phase transition, while the heavy RE (Gd−Yb) ones display magnetic transitions. $YbAu_2In$[19] shows a pressure induced transition from intermediate valence to trivalent magnetic states.[11,15] Further examples are the RE_2Au_2In (RE = La−Gd and RE = Tm−Lu)[20] which adopt two different structure types depending on the size of the RE, Yb_2T_2In (T = Cu, Pd, Au),[21] and $REAg_2In$

*To whom correspondence should be addressed. E-mail: m-kanatzidis@northwestern.edu.

(1) Villars, P.; Calvert, L. D. *Pearson's Handbook of Crystallographic Data for Intermetallic Phases*, 2nd ed.; American Society for Metals: Materials Park, OH, 1991.
(2) Kalychak, Y. M. *J. Alloys Compd.* **1997**, *341*, 262.
(3) Szytoula, A.; Leciejewicz, J. *Handbook of Crystal Structures and Magnetic Properties of Rare Earth Intermetallics*; CRC Press: Boca Raton, FL, 1994.
(4) Rossi, D.; Ferro, R.; Contardi, V.; Marazza, R. *Z. Metallkd.* **1977**, *68*, 493.
(5) Fujii, H.; Uwatoko, Y.; Akayam, M.; Satch, K.; Maeno, Y.; Fujita, T.; Sakurai, J.; Kamimura, H.; Okamoto, T. *Jpn. J. Appl. Phys.* **1987**, *26*, 549.
(6) Szytula, A.; Penc, B.; Gondek, L. *Acta Phys. Pol., A* **2007**, *111*, 475.
(7) Gondek, L.; Szytula, A.; Penc, B.; Hernandez-Velasco, J.; Zygmunt, A. *J. Magn. Magn. Mater.* **2003**, *262*, L177–L180.
(8) Gondek, L.; Penc, B.; Szytula, A.; Jezierski, A.; Zygmunt, A. *Acta Phys. Pol., B* **2003**, *34*, 1209.
(9) Mullmann, R.; Mosel, B. D.; Eckert, H.; Kotzyba, G.; Pottgen, R. *J. Solid State Chem.* **1998**, *137*, 174.
(10) Szytula, A.; Bazela, W.; Gondek, L.; Jaworska-Golab, T.; Penc, B.; Stusser, N.; Zygmunt, A. *J. Alloys Compd.* **2002**, *336*, 11.
(11) Zell, W.; Pott, R.; Roden, B.; Wohlleben, D. *Solid State Commun.* **1981**, *40*, 751.
(12) Bauchspiess, K. R.; Boksch, W.; Holland-Moritz, E.; Launois, H.; Pott, R.; Wohlleben, D. *Proceedings of the International Conference on Valence Fluctuations in Solids*, St. Barbara, U.S.A., 1981.
(13) Pottgen, R. *J. Mater. Chem.* **1996**, *6*, 63.
(14) Oesterreicher, H.; Parker, F. T. *Phys. Rev. B* **1977**, *16*, 5009.
(15) Fuse, A.; Nakamoto, G.; Ishimatsu, N.; Kurisu, M. *J. Appl. Phys.* **2006**, *100*, 043712.
(16) Besnus, M. J.; Kappler, J. P.; Meyer, A.; Sereni, J.; Siaud, E.; Lahiouel, R.; Pierre, J. *Phys. B & C* **1985**, *130*, 240–242.
(17) Besnus, M. J.; Kappler, J. P.; Ravet, M. F.; Mayer, A.; Lahiouel, R.; Pierre, J.; Siaud, E.; Nieva, G.; Sereni, J. *J. Less-Common Met.* **1986**, *120*, 101.
(18) Kurisu, M.; Fuse, A.; Nobata, T.; Nakamoto, G. *Phys. B* **2000**, *281 & 282*, 147.
(19) Muller, D.; Hussain, S.; Cattaneo, E.; Schneider, H.; Schlabitz, W.; Wohlleben, D. *Valence Instabilities*; Wachter, P.; Boppart, H., Eds; North-Holland: Amsterdam, 1982, p 463.
(20) Pottgen, R. *Z. Naturforch B: Chem. Sci.* **1994**, *49B*, 1525.
(21) Giovannini, M.; Bauer, E.; Michor, H.; Hilscher, G.; Galatanu, A.; Saccone, A.; Rogl, P. *Intermetallics* **2001**, *9*, 481–485.

Published on Web 01/19/2011

(RE = Tb, Dy).[22] An especially interesting set of compounds are $YbCu_{4+x}In_{1-x}$[23−26] and their Ag and Au analogs[27] because they show both mixed and intermediate valency characterized by a first-order temperature-induced isostructural valence phase transition as well as valence fluctuations induced by pressure or alloying. They belong to the class of "light" heavy-fermion systems.[28−30] An increase of the In ratio in the RE/Au/In system leads to $Eu_2Au_3In_4$,[31] $RE_2Au_3In_5$ (RE = Ce, Pr, Nd, Sm, Yb),[32] $REAu_2In_4$ (RE = La, Ce, Pr, Nd, Yb),[33] and $EuAuIn_2$.[34]

Indium as a flux has been widely used for the crystal growth of principally known binary or ternary phases.[35−42] It has been little exploited as a synthetic medium compared to Al and Ga,[33,36,43−53] especially for quaternary compounds, although there is now an increasing interest in this approach.[54−63] Our work with In flux includes only a limited number of quaternary phases so far, such as the $RE_4Ni_2InGe_4$ (RE = Dy, Ho, Er, Tm)[62] and $RE_7Co_4InGe_{12}$ (RE = Dy, Ho, Yb).[63]

After the rich chemistry revealed by the thorough examination of the ternary RE/Au/In system, we decided to incorporate also a tetrelide such as Ge in order to search for more complex structures and compositions and to compare with the analogous RE/T/Al/Si or Ge and RE/T/Ga/Ge or Si systems investigated previously.[41−53] Among the rare earth compounds, the Yb-based intermetallics, which are considered as the hole counterparts to the isostructural cerium compounds (i.e., f^{13} vs f^{1} systems), have received considerable attention for the past few years. This interest originates from their ability to exhibit various peculiar properties such as intermediate-valence, heavy fermion or Kondo behavior and unusual magnetism.[64−66] These properties are generally believed to arise from the strong hybridization (interaction) between the localized 4f electrons and the delocalized s, p, and d conduction electrons.[67,68]

Here, we present the new compound $Yb_3AuGe_2In_3$, grown from In flux which crystallizes as an ordered variant of the YbAuIn structure.[4] The synthesis, crystal structure, and the study of the magnetic properties, X-ray absorption near edge spectroscopy (XANES), electrical resistivity, thermoelectric power and heat capacity measurements are reported. These studies suggest that $Yb_3AuGe_2In_3$ is an intermediate or heterogeneous mixed-valence system. Similar studies are also reported for the parent isostructural YbAuIn in an attempt to investigate the similarities and/or differences between the two compounds.

2. Experimental Section

2.1. Reagents. The following reagents were used as purchased without further purification: Yb, (in the form of powder ground

(22) Andre, G.; Bazela, W.; Oles, A.; Szytula, A. *J. Magn. Magn. Mater.* **1992**, *109*, 34–38.
(23) Felner, I.; Nowik, I. *Phys. Rev. B* **1986**, *33*, 617.
(24) Felner, I.; Nowik, I.; Vaknin, D.; Potzel, U.; Moser, J.; Kalvius, G. M.; Wortmann, G.; Schmiester, G.; Hilscher, G.; Gratz, E.; Schmitzer, C.; Pillmayr, N.; Prasad, K. G.; de Waard, H.; Pinto, H. *Phys. Rev. B* **1987**, *35*, 6956.
(25) Nowik, I.; Felner, I.; Voiron, J.; Beille, J.; Najib, A.; du Tremolet de Lachiesserie, E.; Gratz, E. *Phys. Rev. B* **1988**, *37*, 5633.
(26) Sarrao, J. L. *Phys. B* **1999**, *259−261*, 128.
(27) Sarrao, J. L.; Immer, C. D.; Fisk, Z.; Booth, C. H.; Figueroa, E.; Lawrence, J. M.; Modler, R.; Cornelius, A. L.; Hundley, M. F.; Kwei, G. H.; Thompson, J. D. *Phys. Rev. B* **1999**, *59*, 6855.
(28) Mushnikov, N. V.; Goto, T.; Rozenfeld, E. V.; Yoshimura, K.; Zhang, W.; Yamada, M.; Kageyama, H. *J. Phys.: Condens. Matter* **2003**, *15*, 2811.
(29) Junhui, H. E.; Tsujii, N.; Yoshimura, K.; Kosuge, K.; Goto, T. *J. Phys. Soc. Jpn.* **1997**, *66*, 2481.
(30) Golubkov, A. V.; Parfen'eva, L. S.; Smirnov, I. A.; Misiorek, H.; Mucha, J. *Phys. Solid State* **2007**, *49*, 2038–2041.
(31) Hoffmann, R.-D.; Pottgen, R.; Rosenhahn, C.; Mosel, B. D.; Kunnen, B.; Kotzyba, G. *J. Solid Sate Chem.* **1999**, *145*, 283.
(32) Galadzhun, Y. V.; Hoffmann, R.-D.; Pottgen, R.; Adam, M. *J. Solid Sate Chem.* **1999**, *148*, 425.
(33) (a) Salvador, J. R.; Hoang, K.; Mahanti, S. D.; Kanatzidis, M. G. *Inorg. Chem.* **2007**, *46*, 6933. (b) Sebastian, C. P.; Salvador, J.; Martin, J. B.; Kanatzidis, M. G. *Inorg. Chem.* **2010**, *49*, 10468.
(34) Hoffmann, R. D.; Pottgen, R.; Zaremba, V. I.; Kalychak, Y. M. *Z. Naturforch B: Chem. Sci* **2000**, *55*, 834.
(35) Kanatzidis, M. G.; Poettgen, R.; Jeitschko, W. *Angew. Chem., Int. Ed.* **2005**, *44*, 6996–7023.
(36) Salvador, J. R.; Bilc, D.; Gour, J. R.; Mahanti, S. D.; Kanatzidis, M. G. *Inorg. Chem.* **2005**, *44*, 8670–8679.
(37) Canfield, P. C.; Fisk, Z. *Z. Philos. Mag. B* **1992**, *65*, 1117–1123.
(38) Bud'ko, S. l.; Islam, Z.; Wiener, T. A.; Fisher, I. R.; Lacerda, A. H.; Canfield, P. C. *J. Magn. Magn. Mater.* **1999**, *205*, 53–78.
(39) Fisher, I. R.; Islam, Z.; Canfield, P. C. *J. Magn. Magn. Mater.* **1999**, *202*, 1–10.
(40) Nicklas, M.; Sidorov, V. A.; Borges, H. A.; Pagliuso, P. G.; Petrovic, C.; Fisk, Z.; Sarrao, J. L.; Thompson, J. D. *Phys. Rev. B* **2004**, *67*, 020506.
(41) Hundley, M. F.; Sarrao, J. L.; Thompson, J. D.; Movshovich, R.; Jaime, M.; Petrovic, C.; Fisk, Z. *Phys. Rev. B* **2001**, *65*, 024401.
(42) Macaluso, R. T.; Sarrao, J. L.; Moreno, N. O.; Pagliuso, P. G.; Thompson, J. D.; Fronczek, F. R.; Hundley, M. F.; Malinowski, A.; Chan, J. Y. *Chem. Mater.* **2003**, *15*, 1394–1398.
(43) Chen, X. Z.; Sportouch, S.; Sieve, B.; Brazis, P.; Kannewurf, C. R.; Cowen, J. A.; Patschke, R.; Kanatzidis, M. G. *Chem. Mater.* **1998**, *10*, 3202–3211.
(44) Chen, X. Z.; Larson, P.; Sportouch, S.; Brazis, P.; Mahanti, S. D.; Kannewurf, C. R.; Kanatzidis, M. G. *Chem. Mater.* **1999**, *11*, 75–83.
(45) Zhuravleva, M. A.; Kanatzidis, M. G. *Z. Naturforch B: Sect. B* **2003**, *58*, 649–657.
(46) Sieve, B.; Chen, X. Z.; Henning, R.; Brazis, P.; Kannewurf, C. R.; Cowen, J. A.; Schultz, A. J.; Kanatzidis, M. G. *J. Am. Chem. Soc.* **2001**, *123*, 7040–7047.
(47) Zhuravleva, M. A.; Pcionek, R. J.; Wang, X. P.; Schultz, A. J.; Kanatzidis, M. G. *Inorg. Chem.* **2003**, *42*, 6412–6424.
(48) Zhuravleva, M. A.; Evain, M.; Petricek, V.; Kanatzidis, M. G. *J. Am. Chem. Soc.* **2007**, *129*, 3082–3083.
(49) Chen, X. Z.; Small, P.; Sportouch, S.; Zhuravleva, M.; Brazis, P.; Kannewurf, C. R.; Kanatzidis, M. G. *Chem. Mater.* **2000**, *12*, 2520–2522.
(50) Latturner, S. E.; Bilc, D.; Mahanti, S. D.; Kanatzidis, M. G. *Inorg. Chem.* **2003**, *42*, 7959–7966.
(51) Wu, X. U.; Latturner, S. E.; Kanatzidis, M. G. *Inorg. Chem.* **2006**, *45*, 5358–5366.
(52) Latturner, S. E.; Kanatzidis, M. G. *Inorg. Chem.* **2008**, *47*, 2089–2097.
(53) Latturner, S. E.; Bilc, D.; Mahanti, S. D.; Kanatzidis, M. G. *Chem. Mater.* **2002**, *14*, 1695–1705.
(54) Salvador, J. R.; Gour, J. R.; Bilc, D.; Mahanti, S. D.; Kanatzidis, M. G. *Inorg. Chem.* **2004**, *43*, 1403–1410.
(55) Salvador, J. R.; Malliakas, C.; Gour, J. R.; Kanatzidis, M. G. *Chem. Mater.* **2005**, *17*, 1636–1645.
(56) Bailey, M. S.; McCuire, M. A.; DiSalvo, F. J. *J. Solid Sate Chem.* **2005**, *178*, 3494–3499.
(57) Benbow, E. M.; Latturner, S. E. *Inorg. Chem.* **2006**, *179*, 3989–3996.
(58) Klunter, W.; Jung, W. *J. Solid Sate Chem.* **2006**, *179*, 2880–2888.
(59) Zaremba, V. I.; Dubenskiy, V. P.; Rodewald, U. C.; Heying, B.; Pottgen, R. *J. Solid State Chem.* **2006**, *179*, 891–897.
(60) Lukachuk, M.; Galadzhun, Y. V.; Zaremba, R. I.; Dzevenko, M. V.; Kalychak, Y. M.; Zaremba, V. I.; Rodewald, U. C.; Pottgen, R. *J. Solid State Chem.* **2005**, *178*, 2724–2733.
(61) Macaluso, R. T.; Sarrao, J. L.; Pagliuso, P. G.; Moreno, N. O.; Goodrich, R. G.; Browne, D. A.; Fronczek, F. R.; Chan, J. Y. *J. Solid Sate Chem.* **2002**, *166*, 245–250.
(62) Salvador, J. R.; Kanatzidis, M. G. *Inorg. Chem.* **2006**, *45*, 7091–7099.
(63) Chondroudi, M.; Balasubramanian, M.; Welp, U.; Kwok, W.-K.; Kanatzidis, M. G. *Chem. Mater.* **2007**, *19*, 4769–4775.
(64) Kindler, B.; Finsterbusch, D.; Graf, R.; Ritter, F. *Phys. Rev. B* **1994**, *50*, 704.
(65) Bauer, E. *Adv. Phys.* **1991**, *40*, 417.
(66) Wachter, P. *Handbook on the Physics and Chemistry of Rare Earths*; Elsevier Science: Amsterdam, 1994; p 177.
(67) Lawrence, J. M.; Riseborough, P. S.; Park, R. D. *Rep. Prog. Phys.* **1981**, *44*, 1.
(68) Fisk, Z.; Hess, D. W.; Pethick, C. J.; Pines, D.; Smith, J. L.; Thomson, J. D.; Willis, J. O. *Science* **1988**, *239*, 33.

Table 1. Crystallographic Data and Refinement Details for $Yb_3AuGe_2In_3$ and $Yb_3Au_3In_3$

empirical formula	$Yb_3AuGe_2In_3$	$Yb_3Au_3In_3$
formula weight	1205.73	1454.52
temperature (K)	293(2)	293(2)
wavelength (Å)	0.71073	0.71073
crystal system	hexagonal	hexagonal
space group	$P\bar{6}2m$	$P\bar{6}2m$
a, b (Å)	7.3153(8)	7.712(1)
c (Å)	4.4210(5)	4.0294(8)
V (Å^3)/Z	204.89(4)/1	207.58(6)/1
D_{calc} (g/cm^3)	9.772	11.635
absorption coefficient (mm^{-1})/F(000)	67.086/500	94.272/594
θ range for data collection (^{o})	3.22 to 28.25	5.06 to 34.27
index ranges	$-9 \le h \le 9$	$-12 \le h \le 12$
	$-9 \le k \le 9$	$-12 \le k \le 12$
	$-5 \le l \le 5$	$-5 \le l \le 6$
reflections collected/unique/R(int)	2272/213/0.0262	2949/363/0.1339
completeness to θ (%)	99.2	99.5
data/restraints/parameters	213/0/14	363/0/14
refinement method	full-matrix least-squares on F^2	
goodness-of-fit on F^2	1.077	1.192
final R indices [$I > 2\sigma(I)$] (R_1/wR_2)[a]	0.0298/0.0746	0.0418/0.1039
R indices (all data) (R_1/wR_2)[a]	0.0298/0.0746	0.0432/0.1046
extinction coefficient	0.0012(6)	0.0037(9)
largest diff. peak and hole (e. Å^{-3})	1.723 and −1.777	4.004 and −2.994

[a] $R_1 = \Sigma\|F_o| - |F_c\|/\Sigma|F_o|$; w$R_2 = [\Sigma w\{|F_o| - |F_c|\}^2/\Sigma w|F_o|^2]^{1/2}$; $w = 1/\sigma^2\{|F_o|\}$.

from metal chunk, 99.9% Chinese Rare Earth Information center, Inner Mongolia, China), Au (pieces, 99.9% Alfa Aesar, Ward Hill, MA), Ge (ground from 2 to 5 mm pieces 99.999% Cerac, Milwaukee, WI), and In (tear drops 99.99% Plasmaterials, Livermore, CA).

2.2. Synthesis. $Yb_3AuGe_2In_3$ was obtained by combining 3 mmol of the ytterbium metal, 2 mmol of gold, 3 mmol of germanium, and 15 mmol of Indium in an Al_2O_3 (alumina) crucible under an inert nitrogen atmosphere inside a glovebox. The crucible was placed in a 13 mm fused silica tube, which was flame-sealed under vacuum of 10^{-4} Torr, to prevent oxidation during heating. The reactants were then heated to 1000 °C over 10 h, maintained at that temperature for 5 h to allow proper homogenization, followed by cooling to 850 °C in 2 h, and held there for 48 h. Finally, the system was allowed to slowly cool to 50 °C in 48 h. The reaction product was isolated from the excess In flux by heating at 350 °C and subsequent centrifugation through a coarse frit. Any remaining flux was removed by immersion and sonication in glacial acetic acid for 48 h. The final crystalline product was rinsed with water and dried with acetone. This method produced the target compound with ~90% purity and in a yield of ~90% on the basis of the initial amount of Yb metal used in the reaction. Main side products were very small amounts of YbAuGe and residual In metal fux. Several crystals, which grow as metallic silver rods, were carefully selected for elemental analysis, structure characterization, and the physical measurements reported here.

YbAuIn was prepared by mixing 0.1 g of Yb (0.58 mmol), 0.114 g of Au (0.58 mmol), and 0.066 g of In (0.58 mmol). A total of 280 mg was used for the synthesis. The reactants were sealed in tantalum ampules under an argon atmosphere in an arc-melting apparatus. The mixture was heated to around 1100 °C over 11 h and kept there for 24 h, followed by cooling to 50 °C at a rate of −100 °C/h. The yield was 95%, and the sample was observed to be pure up to the level of X-ray detection. A comparison of the experimental powder XRD pattern with the theoretical one derived from the crystal structure refinements indicated very good agreement. The cell parameters obtained from the single crystal XRD refinement and powder XRD are available in Supporting Information. Before the physical measurements, the specimens were additionally (besides the acetic acid) soaked and sonicated with ~6 M of HCl acid to remove any adventitious residues.

2.3. Elemental Analysis. Quantitative microprobe analyses of $Yb_3AuGe_2In_3$ and YbAuIn were performed with a Hitachi S-2700 scanning electron microscope (SEM) equipped with a light-element window Noran System Six energy dispersive spectroscopy (EDS) detector. Data were acquired with an accelerating voltage of 20 kV and a 60 s accumulation time. The EDS analysis taken on visibly clean surfaces of the $Yb_3AuGe_2In_3$ crystals gave the atomic composition of 33% Yb, 11% Au, 33% In, and 23% Ge, which is in very good agreement with the results derived from the single crystal X-ray diffraction refinement. For the mainly polycrystalline YbAuIn, the EDS analysis gave the atomic composition of 35% Yb, 34% Au, and 31% In in fairly good agreement with the single crystal X-ray diffraction results, though some pieces gave Yb rich content, suggesting there may be impurities present.

2.4. X-ray Crystallography. To determine the phase identity and purity, powder X-ray diffraction patterns of $Yb_3AuGe_2In_3$ and YbAuIn were collected at RT on a CPS 120 INEL X-ray diffractometer with Cu Kα radiation, equipped with a position-sensitive detector, and were compared to the pattern calculated from the single crystal structure refinement.

The single crystal X-ray intensity data were collected at room temperature using a STOE IPDS 2T (with additional capability of 2θ swing of the detector) diffractometer with graphite-monochromatized Mo Kα (λ = 0.71073 Å) radiation. The X-AREA (and X-RED and X-SHAPE within) package suite[69] was used for data extraction and integration and to apply empirical and analytical absorption corrections. The structures of $Yb_3AuGe_2In_3$ and YbAuIn single crystals were solved by direct methods and refined with the SHELXTL package of programs.[70] A stable refinement for both compounds was accomplished only in the hexagonal space group $P\bar{6}2m$. Data collection and structure refinement details are given in Table 1. The final atomic positions and equivalent isotropic displacement parameters are listed in Table 2. Table 3 gives a list of selected bond distances for $Yb_3AuGe_2In_3$ and YbAuIn.

2.5. Magnetic Measurements. Magnetic susceptibility measurements for $Yb_3AuGe_2In_3$ and YbAuIn were carried out with a Quantum Design MPMS SQUID magnetometer. The crystals

(69) GmbH, STOE & CIE D 64295; Darmstadt, Germany, 2006.
(70) Bruker, Advanced X-ray Solutions SHELXTL (Version 6.14); Bruker AXS Inc., Madison, WI, 2003.

Table 2. Atomic Coordinates ($\times 10^4$) and Equivalent Isotropic Displacement Parameters (Å^2 $\times 10^3$) for $Yb_3AuGe_2In_3$ and $Yb_3Au_3In_3$

atom	Wyckoff	*x*	*y*	*z*	U_{eq}[a]
		$Yb_3AuGe_2In_3$			
Yb	3*g*	4197(2)	0	5000	9(1)
Au	1*b*	0	0	5000	15(1)
Ge	2*c*	3333	−3333	0	8(1)
In	3*f*	7512(3)	0	0	13(1)
		YbAuIn			
Yb	3*g*	4069(2)	0	5000	11(1)
Au(1)	1*b*	0	0	5000	12(1)
Au(2)	2*c*	3333	−3333	0	11(1)
In	3*f*	7416(3)	0	0	10(1)

[a] U(eq) is defined as one-third of the trace of the orthogonalized U^{ij} tensor.

Table 3. Selected Bond Lengths (Å) for $Yb_3AuGe_2In_3$ and $Yb_3Au_3In_3$

bond	$Yb_3AuGe_2In_3$	$Yb_3Au_3In_3$
Yb−Au/Yb-Au(1)	3.070(1)	3.0874(5)
Yb−In	3.281(2)	3.275(2)
	3.4694(9)	3.409(1)
Yb−Ge	3.1131(4)	
Yb−Au(2)		3.0874(5)
Au−In/Au(1)-In	2.863(1)	2.8340(1)
Au(2)-In		2.903(1)
Ge−In	2.799(1)	
Yb−Yb	3.7966(8)	4.052(1)

used for the data collection were ground in open air atmosphere. Temperature dependence data were collected between 3 and 400 K, for both zero field cooled and field cooled mode, with an applied field of 500 and 1000 G for $Yb_3AuGe_2In_3$ and YbAuIn, respectively. Field dependent magnetic measurements were acquired at 3 and 150 K with field sweeping from 0 up to 50 kG. Core diamagnetic corrections were applied. In order to study the magnetic anisotropy of the material, temperature dependent measurements were performed on several aligned single crystals oriented with the *c*-axis parallel and normal to the applied field of 2 kG. Field dependence measurements were also performed for both orientations at 5 K between 0 and 50 kG.

2.6. X-ray Absorption near Edge Spectroscopy (XANES). X-ray absorption near edge spectroscopy (XANES) experiments were performed in Sector 20, bending magnet beamline (PNC/XOR, 20-BM) of the Advanced Photon Source. Measurements at the Yb L_{III} edge and at ambient pressure were performed in transmission mode using gas ionization chambers to monitor the incident and transmitted X-ray intensities. A third ionization chamber was used in conjunction with a copper foil to provide internal calibration for the alignment of the edge positions. Monochromatic X-rays were obtained using a Si (111) double crystal monochromator. The monochromator was calibrated by defining the inflection point (first derivative maxima) of Cu foil as 8980.5 eV.[71] A rhodium-coated X-ray mirror was utilized to suppress higher order harmonics. The $Yb_3AuGe_2In_3$ and YbAuIn samples were prepared by mixing an appropriate amount of finely ground powder with boron nitride and cold pressing them to a pellet as well as by dusting the finely ground sample on Kapton tape and stacking several layers (8−12 layers) together. Most of the sample preparation procedures were carried out inside a nitrogen glovebox environment. Measurements were performed at a range of temperatures from 15 to 300 K using a closed cycle refrigerator. Data reduction and analysis were performed using Athena and Artemis software developed by Newville and Ravel.[72] Care was taken to minimize thickness effects in the measurements.

2.7. Resistivity, Heat Capacity, and Thermopower. For $Yb_3AuGe_2In_3$, electrical resistivity was determined using a six probe technique in a standard ^{4}He gas flow cryostat. Heating was avoided by reducing the current, and hysteresis, caused by slight thermometer−sample temperature differences, was avoided by sweeping the temperature slowly. More detailed experimental description can be found elsewhere.[73] Data points were taken during the cooling cycle from 302 to 2.48 K. The typical size of the $Yb_3AuGe_2In_3$ rod-shaped crystals measured was 0.66 × 0.12 × 0.08 mm.

For YbAuIn, electrical resistivity was measured as a function of temperature on single crystals. Electrical contact was made using silver paint and Cu wire directly on the crystals surface. Measurements were made for arbitrary current directions in the *a*,*c*-plane using a standard four point contact geometry (AC) in a quantum design physical property measurement system (PPMS). Data points were recorded during the heating cycle at a temperature range of 1.8−274.3 K. The typical size of the YbAuIn rod-shaped crystals measured was 2.5 × 1 × 0.6 mm.

Specific heat measurements of single crystals of $Yb_3AuGe_2In_3$ and YbAuIn were performed on a Quantum Design PPMS commercial device in the temperature range of 1.8−50.3 K by relaxation method using the "Two-Tau Model".[74] Thermoelectric power was measured using a SB-100 Seebeck measurement system in the temperature range between 310 and 710 K on a single rod-shaped crystal of $Yb_3AuGe_2In_3$. The electrical contact for the thermopower measurement was made using silver paint with the sample mounted on an alumina stage.

3. Results and Discussion

3.1. Reaction Chemistry. Crystals of $Yb_3AuGe_2In_3$ grow in indium flux generally as metallic silver rods and in a smaller portion as thinner needles. Figure 1A shows a SEM image of a typical rod type $Yb_3AuGe_2In_3$ crystal. Reaction byproducts were small amounts of unreacted gold which tends to wet the surface of the crystals as well as very small amounts of YbAuGe, which due to very different crystal morphology (polygonal shape) could be easily distinguished and removed when necessary. When other rare earth metals such as Ce, Sm, Eu, Dy, and Pr were employed under the same reaction conditions, we did not observe analogs of $Yb_3AuGe_2In_3$. In contrast, the REAuIn family of compounds forms with most of the RE atoms including Yb.[4]

The YbAuIn compound was synthesized by direct combination of the reactants in primarily gray polycrystalline form and pieces made up from packed crystals, with the exception of the formation of a few needlelike single silvery metallic crystals. The main byproduct was recrystallized Ta from the reaction vessel. Attempts to generate the YbAuIn phase in high purity and yield by flux reactions failed because of several competing $Yb_xAu_zIn_y$ phases. Figure 1B depicts an SEM image of a typical YbAuIn chunk. Both compounds are stable in air and no decomposition was observed for weeks.

Given that YbAuIn and $Yb_3AuGe_2In_3$ are structurally related, one would expect that there may be some phase width to $Yb_3AuGe_2In_3$. Although we did not do an exhaustive study of this issue, we have not observed any

(71) Kraft, S.; Stumpel, J.; Becker, P.; Kuetgens, U. *Rev. Sci. Instrum.* **1996**, *67*, 681.

(72) Ravel, B.; Newville, M. *J. Synchrotron Radiat.* **2005**, *12*(4), 537–541.

(73) Li, Q. A.; Gray, K. E.; Mitchell, J. F. *Phys. Rev. B* **1999**, *59*, 9357–9361.

(74) *Advanced Heat Capacity with Helium-3 Application Note. Physical Property Measurement System Brochure*, 1999.

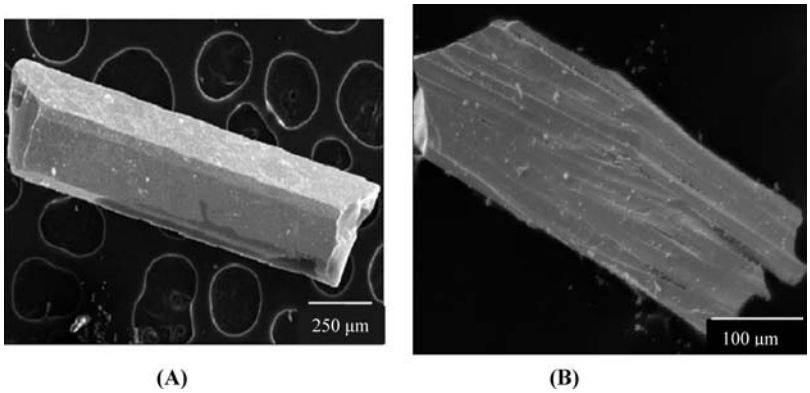

Figure 1. Scanning electron micrograph (SEM) image of (A) a flux-grown $Yb_3AuGe_2In_3$ single crystal and (B) a compact piece of YbAuIn.

evidence of solid solution behavior of the type $Yb_3Au_{3-x}Ge_xIn_3$. The lattice parameters as judged by a comparison of powder diffraction patterns from the various batches and the derived lattice parameters from the various samples did not show the type of Bragg line shifts that would be suggestive of this. In addition, we made attempts to synthesize $Yb_3Au_2GeIn_3$ (where only one Ge atom substitutes for Au instead of two, i.e., where $x = 1$ in $Yb_3Au_{3-x}Ge_xIn_3$). The results were negative for the existence of $Yb_3Au_2GeIn_3$ as judged by powder X-ray diffraction. We did not, however, investigate any compositions which are close to the $Yb_3AuGe_2In_3$. Therefore, we cannot definitely state that $Yb_3AuGe_2In_3$ is a line compound.

3.2. Crystal Structure. YbAuIn and $Yb_3AuGe_2In_3$ adopt the ZrNiAl-type structure,[75] which itself is a ternary ordered version of the aristotype structure of Fe_2P,[76] in the hexagonal space group $P\bar{6}2m$. $Yb_3AuGe_2In_3$ crystallizes as an ordered variant of the YbAuIn structure.[4,11] YbAuIn contains two crystallographically independent gold sites in trigonal prismatic coordination. In the quaternary compound, Ge substitutes in the Au2 position (2*c* wyckoff site, see Table 2) of the parent compound written as $Yb_3Au_3In_3$. The overall structure of the quaternary compound as viewed down the *c*-axis is illustrated in Figure 2. The Au atoms have trigonal prisms formed by the In atoms and those of Ge are built up from ytterbium atoms. Both types of trigonal prisms are capped on the rectangular faces: [$AuIn_6$] by three ytterbium atoms and [$GeYb_6$] by three indium atoms, leading to coordination number nine for gold and germanium sites, Figure 3. The In atom is eight coordinate, bonded to two other In atoms as well as to two Au, Yb, and Ge atoms, respectively, in an arrangement that could be described as distorted tetragonal prism, Figure 3. The coordination environment of the crystallographically unique Yb site is defined by six In atoms and four Ge atoms that give rise to a pentagonal prismatic geometry, capped by a single Au atom, Figure 3.

The bond between the In atoms is 3.152(4) Å which compares well to the In−In bonds found in $REAu_2In_4$[33] ranging between 2.966(1) and 3.172(1); but it is shorter than the average In−In distance of 3.333 Å in elemental In,[77] suggesting rather strong bonding. The In−Ge bonds

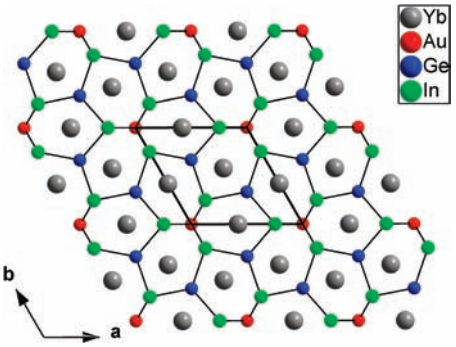

Figure 2. Overall structure of $Yb_3AuGe_2In_3$ as viewed down the *c*-axis. For clarity, the bonds to the Yb atoms are not drawn.

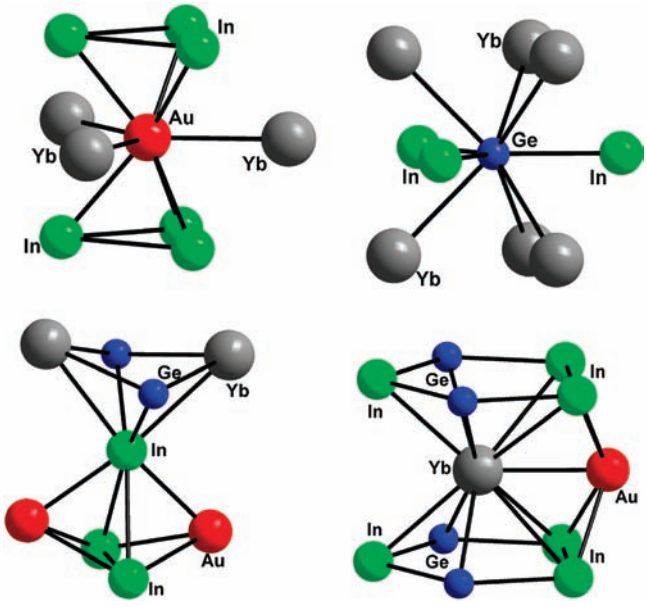

Figure 3. Coordination environment of the Au, Ge, In, and Yb atoms. The coordination sphere cutoff is 3.5 Å.

at 2.7993(14) compare well to corresponding distances found in EuInGe[78] and $Ca_2LiInGe_2$[79] ranging from 2.75 to 2.876 Å, but these are shorter than the ones found in the quaternary phase $RE_7Co_4InGe_{12}$[63] (ranging from

(75) Yoshida, M.; Akiba, E.; Shimojo, Y.; Morii, Y.; Izumi, F. *J. Alloys Compd.* **1995**, *231*, 755.
(76) Hendricks, S. B.; Kosting, P. R. *Z. Kristallogr.* **1930**, *74*, 511.
(77) Donohue, J. *The structures of the elements*; Wiley: New York, 1974.
(78) Mao, J.-G.; Goodey, J.; Guloy, A. M. *Inorg. Chem.* **2002**, *41*, 931–937.
(79) Mao, J.-G.; Xu, Z.; Guloy, A. M. *Inorg. Chem.* **2001**, *40*, 4472–4477.

2.9214(14) to 2.965(3) Å) or in $Ce_3In_{0.89}Ge_{1.11}$[80] where they have the value of 2.99 Å.

The three-dimensional arrangement that the rare earth atoms adopt in this structure type leads to three exceptional features: (i) The RE ions within the same layer form triangles, so when it comes to antiferromagnetic coupling between nearest neighbors, this topology can cause frustration of the magnetic interactions. (ii) The fact that the magnetic RE atoms are stacked in $[Yb_3Au]$ layers that alternate with the nonmagnetic $[Ge_2In_3]$ layers can give rise to indirect exchange interactions. (iii) The crystalline electric field surrounding the lanthanide ions frequently induces strong anisotropy, which leads either to Ising or XY spin behavior.[81,82] Examples of compounds adopting this arrangement are the families of REAuIn[10−12] and RENiAl.[83,84] The Au atoms are isolated from one another and are found among the Yb triangles in the net at a Au−Au distance of 7.3153(8) Å, which is equal to the *a*-cell parameter. With respect to the $[Ge_2In_3]$ slab, the $[Yb_3Au]$ layer is positioned so that the Yb atoms are aligned with the centers of the pentagons, while the Au atoms are in registry with the In triangles; see Figure 2.

A comparison between the crystal structure parameters ($a = b$ and c in the hexagonal coordinate system) of these two compounds reveals an interesting feature: the *a*-parameter of $Yb_3Au_3In_3$ is larger than that of $Yb_3AuGe_2In_3$ which is related to the fact that Au is larger than Ge. On the other hand, it is striking that the *c*-parameter of $Yb_3Au_3In_3$ is ~10% shorter than that of $Yb_3AuGe_2In_3$ (see Table 1) which cannot be explained by the size difference between Au and Ge. This *c*-axis contraction may reflect a stronger Yb−Au bonding interaction in YbAuIn compared to the Yb−Ge interaction in $Yb_3AuGe_2In_3$. This difference in bonding may reflect the marked difference in electronegativity between Yb (1.1) and Au (2.54) vis-à-vis Yb (1.1) and Ge (2.0) (Pauling scale). Since the Yb−Ge interactions are along the *c*-axis of the structure, presumably the lower degree of bonding between Yb and Ge1 in $Yb_3AuGe_2In_3$ compared to Yb−Au in YbAuIn would result in weaker bonding and longer *c*-axis length. First principles theoretical calculations would be useful here in shedding further light into the local bonding in these materials.

3.3. Magnetism. Figure 4A shows the temperature dependence of the molar magnetic susceptibility (χ_m) of a ground sample of $Yb_3AuGe_2In_3$ measured from 3 to 400 K with applied field of 500 G. The magnetic susceptibility data follow a modified Curie−Weiss (CW) law that includes a temperature independent component according to the equation $\chi(T) = \chi_0 + C/(T - \theta_p)$. χ_o includes the sum of the temperature independent contributions, e.g., van Vleck paramagnetism and Pauli paramagnetism (due to conduction electrons). The effective magnetic moment μ_{eff} was deduced from the Curie constant C, ($C = \mu_{eff}^2/8$). A nonlinear least-squares fit to this equation resulted in

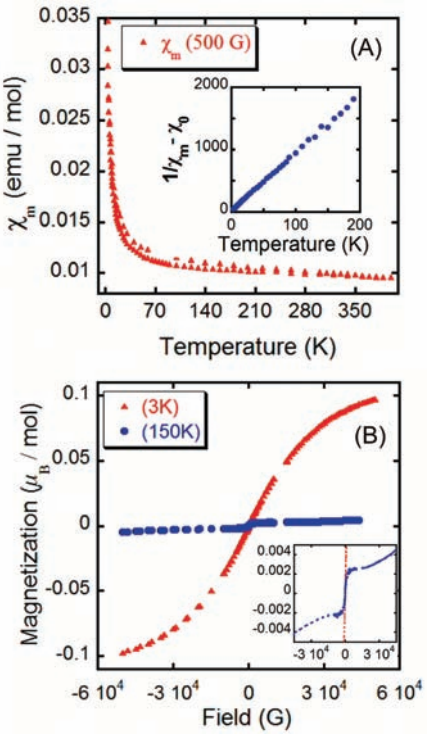

Figure 4. (A) Temperature dependence of the molar susceptibility χ_m of $Yb_3AuGe_2In_3$ (ground sample) with an applied field of 500 G. The inset shows the plot of $1/(\chi_m - \chi_0)$ versus temperature. (B) Magnetization data of $Yb_3AuGe_2In_3$ collected at 3 and 150 K.

$\chi_0 = 3.2 \times 10^{-3}$ emu/mol of Yb atom, Curie−Weiss constant of $\theta_p = -1.5$ K, indicating antiferromagnetic interactions and an effective moment of 0.52 μ_B/Yb atom. The inset in Figure 4A shows the plot of $1/(\chi - \chi_0)$ versus temperature. The estimated effective moment of 0.52 μ_B is only ~11.5% of the value expected for the free-ion Yb^{3+}, 4.54 μ_B. This indicates that the compound contains both Yb^{2+} and Yb^{3+} species. In order to confirm the presence of Yb^{3+} species in the title compound, we performed XANES studies that are discussed below.

The field dependence of the magnetization $M(H)$ for a ground sample of $Yb_3AuGe_2In_3$ at 3 and 150 K are shown in Figure 4B. The data at 3 K exhibit linear behavior up to about 12 kG at which point the slope changes continuously until ~33 kG, and then, it becomes linear again but with a much shallower slope. No signs of saturation up to the highest attainable field of 50 kG were observed. The magnetization curve taken at 150 K showed a very different picture. There is a strong field dependent response up to ~1.2 kG, which saturates at ~11 kG, while above that field $M(H)$ becomes linear up to the highest obtainable field. This suggests that there is probably a small ferromagnetic component in the $Yb_3AuGe_2In_3$ sample which may be part of the structure itself; however, we cannot rule out the fact that it may also be an extrinsic impurity. If it is an extrinsic impurity phase, the standard techniques such as X-ray diffraction and EDS analysis could not pick it up. It may, however, be nanoinclusions in the body of the crystals which will require detailed transmission electron microscopy (TEM) analysis to investigate, which is beyond the scope of the present work. If on the other hand it is intrinsic, it is possible that there are small domains in the structure that are occupied by

(80) Nychyporuk, G. Z., V.; Kalychak, Ya.M.; Stepien-Damm, J.; Pietraszko, A. *J. Alloys Compd.* **2000**, *312*, 154.
(81) Kawamura, H. *J. Phys.: Condens. Matter* **1998**, *10*, 4707–4754.
(82) Yoshida, H.; Ahlert, S.; Jansen, M.; Okamoto, Y.; Yamaura, J.-I.; Hiroi, Z. *J. Phys. Soc. Jpn.* **2008**, *77*, 074719.
(83) Ehlers, G.; Maletta, H. *Z. Phys. B* **1996**, *101*, 317–327.
(84) Javorsky, P.; Tuan, N. C.; Divis, M.; Havela, L.; Svoboda, P.; Sechovsky, V.; Hilscher, G. *J. Magn. Magn. Mater.* **1995**, *140−144*, 1139.

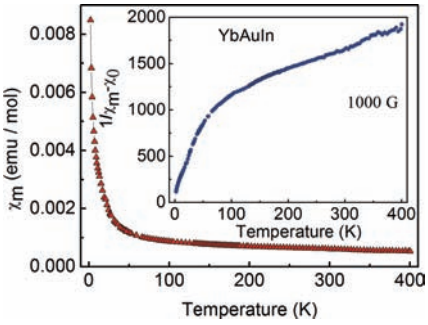

Figure 5. Temperature dependence of the molar susceptibility χ_m of a ground in open air YbAuIn sample, with an applied field of 1 kG. The inset shows the temperature dependent inverse susceptibility of YbAuIn.

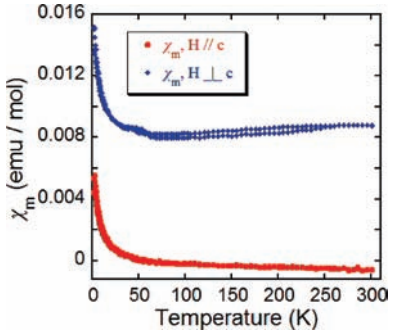

Figure 6. Temperature dependence of the molar susceptibility χ_m of $Yb_3AuGe_2In_3$ on single crystals, oriented with the *c*-axis parallel (red circles) and normal (blue rhombi) to the applied field of 2 kG.

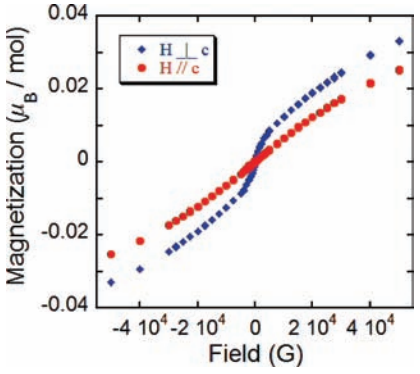

Figure 7. Field dependence magnetization measurements for both parallel and normal orientations to the *c*-axis measured at 5 K between −50 and 50 kG of applied fields.

$Yb^{2+/3+}$ or Yb^{3+} atoms, giving rise to local ferromagnetic moments. Additional investigations will be needed to address this issue.

Figure 5 shows the temperature dependence of the molar magnetic susceptibility (χ_m) of a ground sample of YbAuIn measured from 2 to 400 K and with an applied field of 1 kG. Qualitatively, the $\chi_m(T)$ data display similar behavior with the isostructural $Yb_3AuGe_2In_3$. The inverse molar magnetic susceptibility data $1/(\chi - \chi_0)$ versus temperature is shown as an inset in Figure 5. The inverse susceptibility follows modified CW law only in the temperature region above 100 K. At lower temperatures, the deviation can be attributed to crystal-field contributions and/or to a possible onset of a valence fluctuation. Above 100 K, YbAuIn exhibits paramagnetic behavior with an effective moment of 1.21 μ_B/Yb atom and Curie−Weiss constant of $\theta_p = -409$ K, indicating antiferromagnetic interactions. The estimated experimental μ_{eff} value is about 26% of that expected for a free Yb^{3+} ion (4.54 μ_B). This observed valence for Yb in YbAuIn 2.26 is in agreement with the reported value of 2.18[11] and the XANES measurements (2.22, see below). The slightly larger value of Yb valence in our sample is probably due to the presence of small amount of trivalent oxide (Yb_2O_3) impurity which has been observed before[11] and also confirmed by the XANES measurements. Below 100 K, the $\chi_m(T)$ data do not obey CW law and below ∼80 K there is a slight deviation from linearity. Both susceptibility and low temperature magnetization measurements of YbAuIn exhibit similar behavior with the corresponding ground sample of $Yb_3AuGe_2In_3$.

The 3D arrangement of the RE atoms in the ZrNiAl-structure type often induces strong anisotropy that could lead to interesting phenomena such as Ising or XY spin behavior.[10,83] In order to check this, we measured the magnetic susceptibility parallel and normal to the *c*-axis of crystals of $Yb_3AuGe_2In_3$. Several single crystals were aligned together, so their *c*-axes were nearly parallel. From Figure 6, it is clear that the material is indeed magnetically anisotropic. When the *c*-axis is oriented parallel to the applied field, the material appears nearly diamagnetic above 60 K while when it is aligned normal to the field it exhibits almost temperature independent (Pauli paramagnetic like) behavior which tends to a small increase toward higher temperatures.

The magnetization curve measured at 5 K, see Figure 7, for the parallel orientation to the *c*-axis, shows linear dependence up to 22 kG. Beyond this point, the slope starts to change with no saturation up to 50 kG. Finally, the magnetization with the field normal to *c*-axis is higher in magnitude and exhibits linear response up to 2 kG, followed by a change in slope at ∼4 kG. The moment at 50 kG is 0.08 μ_B/mol more than the corresponding one of the parallel orientation.

3.4. XANES. To further probe the Yb valence state in $Yb_3AuGe_2In_3$ and YbAuIn, we performed X-ray absorption measurements at the Yb L_{III}-edge. The near-edge spectra for both compounds obtained at temperatures of ∼15−18 and 300 K and at ambient pressure showed no significant difference between the two temperatures, suggesting that the Yb valence remained stable in the measured temperature range. The spectra at 295 and 300 K (room temperature) for $Yb_3AuGe_2In_3$ and YbAuIn, respectively, are given in Figure 8. The main absorption peak (white line resonance) of the spectrum for both spectra is centered at ∼8941.5 eV, which is attributed to divalent Yb atoms.[85−87] The spectra also revealed the presence of a weaker feature (shoulder) at ∼8949.5 eV, indicating that some trivalent Yb is also present.[85−87] Since in both compounds under study there is only one unique crystallographic

(85) Rao, C. N. R.; Sarma, D. D.; Sarode, P. R.; Sampathkumaran, E. V.; Gupta, L. C.; Vijayaraghavan, R. *Chem. Phys. Lett.* **1980**, *76*, 413–415.
(86) Hatwar, T. K.; Nayak, R. M.; Padalia, B. D.; Ghatikar, M. N.; Sampathkumaran, E. V.; Gupta, L. C.; Vijayaraghavan, R. *Solid State Commun.* **1980**, *34*, 617–620.
(87) Moreschini, L.; Dallera, C.; Joyce, J. J.; Sarrao, J. L.; Bauer, E. D.; Fritsch, V.; Bobev, S.; Carpene, E.; Huotari, S.; Vanko, G.; Monaco, G.; Lacovig, P.; Panaccione, G.; Fondacaro, A.; Paolicelli, G.; Torelli, P.; Grioni, M. *Phys. Rev. B* **2007**, 75.

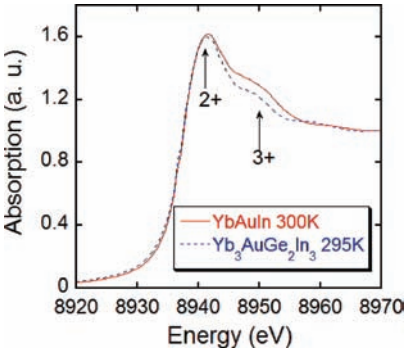

Figure 8. First derivative L_{III} absorption edge spectra of Yb in $Yb_3AuGe_2In_3$ at 295 K (dashed line) and in YbAuIn at 300 K (solid line).

Yb site (as determined by the time scale of diffraction), there could be two plausible scenarios; one in which $Yb_3AuGe_2In_3$ and YbAuIn could be classified as intermediate valence compounds with all Yb atoms having a noninteger valence, and a second where the materials are heterogeneous mixed-valence compounds, in which the Yb atoms alternate between 2+ and 3+ state in various domains.

The relative amounts of the two electronic configurations were determined by decomposing the normalized Yb XANES into a pair of arc-tangents (representing the edge step) and Lorentzians functions (representing the white line resonance). Fitting of the data with the above technique for $Yb_3AuGe_2In_3$ resulted in ~85.2% of Yb^{2+} and ~14.8% of Yb^{3+} which leads to an average Yb valence of ~2.15. For YbAuIn, similar analysis led to an average Yb valence of ~2.22. This is in agreement with the magnetic susceptibility data for this compound discussed above. In the case of YbAuIn, however, while the majority of the Yb is present in the intermediate state, a careful inspection and analysis of the EXAFS indicates that the sample might also contain ~3−5% of a trivalent oxide impurity component. Taking into account the possible presence of an oxide component, we determine the intrinsic valence of Yb in YbAuIn to be ~2.17. This observation is consistent with Yb valence obtained from the magnetic measurements (2.18) by Zell et al.[11] Within the accuracy of the EXAFS technique, the $Yb_3AuGe_2In_3$ sample did not show any noticeable oxide component. We estimate the uncertainty in the absolute valence to be ~5%, arising mainly from correlations between parameters used to represent the edge-step and white line resonances. The Yb^{3+} fraction for $Yb_3AuGe_2In_3$ is consistent with that estimated independently from the magnetic measurements described above.

3.5. Resistivity. The $Yb_3AuGe_2In_3$ compound is clearly metallic. The temperature variation of the electrical resistivity $\rho(T)$ of $Yb_3AuGe_2In_3$ between 2.48 and 302.3 K is presented in Figure 9. The resistivity data measured on single crystals along the *c*-axis and at zero applied field reveal metallic conductivity with a room temperature resistivity value ρ(300K) of 39.6 $\mu\Omega$ cm. When a magnetic field of 6 T was applied, the compound showed no magnetoresistance. In the measured temperature range, the resistivity

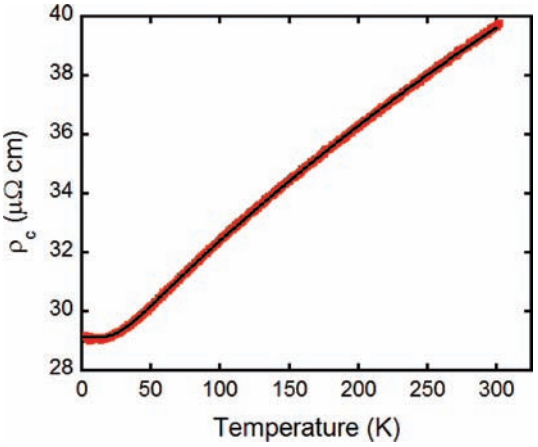

Figure 9. Temperature variation of the electrical resistivity $\rho(T)$ of $Yb_3AuGe_2In_3$ from 2.48 to 302.3 K. The dashed line is a fit of the experimental data (squares) to the Bloch−Grüneisen−Mott formula 2.

of $Yb_3AuGe_2In_3$ can be well described by the Bloch−Grüneisen−Mott (BGM) formula:[88]

$$\rho(T) = \rho_0 + 4R\Theta_D\left(\frac{T}{\Theta_D}\right)^5 \int_0^{\frac{\Theta_D}{T}} \frac{x^5\,dx}{(e^x-1)(1-e^{-x})} - KT^3 \quad (1)$$

where ρ_0 is the residual resistivity, the second term represents electron−phonon scattering, and the third term accounts for Mott's s−d interband electron scattering. The least-squares fitting procedure of (1) yielded the parameters $\rho_0 = 29\ \mu\Omega$ cm and a Debye temperature $\Theta_D = 166$ K, which is in good agreement with the Θ_D value that was estimated from the specific heat results (see below). The relatively low Θ_D is consistent with the presence of heavy atoms in the structure and suggests a soft lattice.

The temperature dependent data of the electrical resistivity $\rho(T)$ of YbAuIn measured between 4.2 and 274.3 K and, at zero applied field, are given in Figure 10. The resistivity, measured on crystals along the *c*-axis, reveals metallic behavior with ρ(274.3K) ~ 433 $\mu\Omega$ cm and ρ_0 ~ 60 $\mu\Omega$ cm, but attempts to fit the $\rho(T)$ data of YbAuIn with the BGM formula 1 were unsuccessful, in contrast to $Yb_3AuGe_2In_3$. The large residual resistivity ratio, RRR, of YbAuIn (RRR ~ 7 compared to 1.36 for $Yb_3AuGe_2In_3$) is often the sign of a cleaner metal with smaller disorder scattering and lower ρ_0. However, ρ_0 is larger in YbAuIn, and then, the much larger temperature dependent resistivity, $\rho(274.3\ \text{K}) - \rho_0$, ~373 $\mu\Omega$ cm, is very hard to reconcile with only electron−phonon and electron−electron scattering, as in the BGM formula. A possible explanation is stronger hybridization of conduction electrons with the localized f electrons of the Kondo lattice of Yb in YbAuIn. In Kondo lattices, this hybridization greatly increases the density of conduction election states and, thus, reduces the resistivity. However, at higher temperatures, entropy considerations decouple these electrons,[89] so the density of states decreases and the resistivity increases. Such an effect goes beyond the BGM assumptions. Note that this coupling also increases the electron's effective mass at low temperatures,

(88) Mott, N. F.; Jones, H. *The Theory of the Properties of Metals and Alloys*; Oxford University Press: New York, 1958; Vol., p 240.

(89) Gegenwart, P.; Si, Q.; Steglich, F. *Nat. Phys.* **2008**, *4*, 186–197.

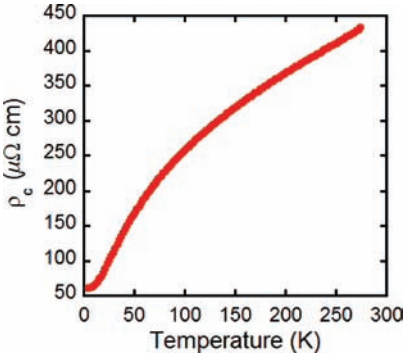

Figure 10. Temperature variation of the electrical resistivity $\rho(T)$ of YbAuIn from 4.2 to 274.3 K and at zero applied field.

leading to a large linear term, γ, in the specific heat that is associated with heavy-fermion behavior. Thus, this idea is consistent with the larger specific heat γ for YbAuIn that implies a "light" heavy-fermion material (see below).

The temperature dependence of the thermoelectric power (TEP) of $Yb_3AuGe_2In_3$ was measured in the temperature range of 310−700 K, (not shown). During the whole temperature, TEP is very small and negative with a magnitude of $-3\ \mu$V/K at room temperature. The negative sign of thermopower is suggestive of the intermediate valence state of the Yb atoms in $Yb_3AuGe_2In_3$ and agrees with the negative TEP observed in most of the Yb-containing mixed- or intermediate-valence compounds, as in YbCuGa[90] and $YbNi_4Si$,[91] for example.

3.6. Heat Capacity. The temperature dependent specific heat from 1.8 to 50 K for $Yb_3AuGe_2In_3$ is shown in Figure 11A. The data can be described well by a Debye function (2) where the first and second term correspond to the electronic and the phonon contribution, respectively. N is the number of the atoms in the formula unit and $x = \hbar\omega/k_BT$.

$$C_p(T) = \gamma T + 9NR\left(\frac{T}{\Theta_D}\right)^3 \int_0^{\frac{\Theta_D}{T}} \frac{x^4\,dx}{(e^x-1)^2} - KT^3 \quad (2)$$

A fit to the experimental points resulted in a Debye temperature Θ_D of about 178 K and an electronic specific heat coefficient $\gamma \approx 31$ mJ/mol K^2, which was determined from $\gamma\ (= C_p/T)_{T\to 0}$ at low temperatures. The observed Θ_D value is slightly higher than the value obtained from the resistivity measurements (166 K).Therefore, the compound does not appear to be a heavy-fermion material according to the arbitrary classification of these compounds into "light", "moderate", and classical heavy-fermions with γ values lying in the range of ~50−60, 100−400, and >400 mJ/mol K^2, respectively. Nevertheless, this value of electronic specific heat compares well with the ones found in other mixed valent or intermediate compounds such as

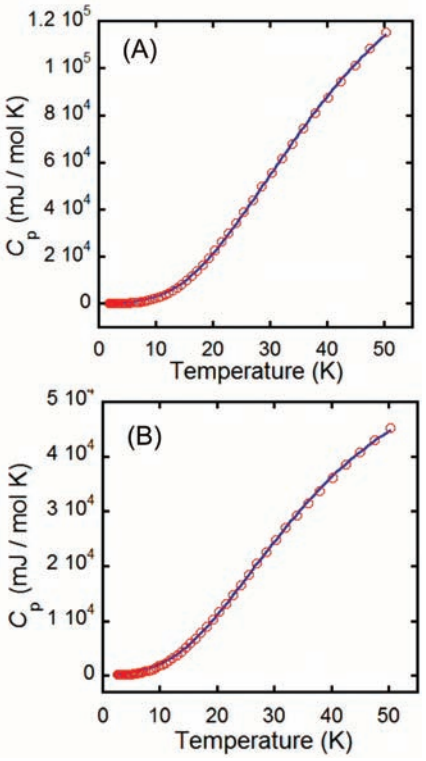

Figure 11. Heat capacity (C_p) of $Yb_3AuGe_2In_3$ (A) and YbAuIn (B) measured from 1.8 to 50.3 K. The experimental data (circles) are fitted with Debye formula 2 (solid line).

the $YbAl_2$,[92] $YbAl_3$,[93] $YbMgCu_4$,[30] $YbNi_4Si$,[91] and $YbInAu_2$[94] in which γ ranges at 15−62 mJ/mol K^2.

The temperature dependent specific heat data measured at a temperature range of 1.8 to 50 K for YbAuIn are shown in Figure 11B. The data can also be described well by the Debye function 2. A least-squares fit to the experimental points resulted in a Debye temperature Θ_D of about 156 K and an electronic specific heat coefficient $\gamma \approx 84$ mJ/mol K^2, which was determined from $\gamma\ (= C_p/T)_{T\to 0}$ at low temperatures. According to the arbitrary classification of the heavy-fermion compounds mentioned above, YbAuIn could be classified as a "light" heavy-fermion compound.

4. Concluding Remarks

The stabilization of $Yb_3AuGe_2In_3$ as an ordered variant of YbAuIn is certainly unanticipated if we consider how different Ge and Au atoms really are. These differences extend over many aspects such as chemical nature, electron count, electronegativity and size. The $Yb_3AuGe_2In_3$ and YbAuIn pair of compounds is, therefore, a rare example of isostructural Ge for Au substitution. We can conclude that the stabilization of the hexagonal structure motif of YbAuIn is not very sensitive to a total electron count. Because of this we can hypothesize that a whole family of isostructural compounds of the type $Yb_3AuM_2In_3$, where M is various metals and metalloids, may exist. Guided by the work reported, it would be interesting to see if some of these predicted compounds can be prepared.

Acknowledgment. This work was supported by UChicago Argonne, LLC, Operator of Argonne National Laboratory.

(90) Androja, D. T.; Malik, S. K.; Padalia, B. D.; Bhatia, S. N.; Walia, R.; Vijayaraghvan, R. *Phys. Rev. B* **1990**, *42*, 2700.
(91) Kowalczyk, A.; Falkowski, M.; Tolinski, T.; Tran, V. H.; Miiller, W.; Reiffers, M.; Timko, M. *Mater. Res. Bull.* **2008**, *43*, 185.
(92) Gorlach, T.; Pfleiderer, C.; Grube, K.; Lohneysen, H. v. *Phys. Rev. B* **2005**, *71*, 033101.
(93) Klaasse, J. C. P.; de Boer, F. R.; de Chatel, P. F. *Phys. B* **1981**, *106*, 178.
(94) Tsujii, N.; Yoshimura, K.; Kosuge, K. *J. Phys.: Condens. Matter* **2003**, *15*, 1993.

Argonne, a U.S. Department of Energy Office of Science Laboratory, operated under Contract DE-AC02-06CH-11357. PNC/XOR facilities and research at these facilities are supported by the U.S. DOE and its founding. We thank Dr. Igor Aronson for his help in developing and analyzing the Formulas 1 and 2 and Dr. Iliya Todorov for his help in the synthesis of YbAuIn, both from the Material Science Division at ANL. Financial support from the Department of Energy (Grant DE-FG02-07E-R46356) is gratefully acknowledged.

Supporting Information Available: Cell parameters obtained from the single crystal XRD refinement and powder XRD. This material is available free of charge via the Internet at http://pubs.acs.org.